Chinese Chemical Letters 36 (2025) 110077

Contents lists available at ScienceDirect

Chinese Chemical Letters

journal homepage: www.elsevier.com/locate/cclet

Tracing molecular margins of lung cancer by internal extractive electrospray ionization mass spectrometry

Haiyan Lu[a,b], Jiayue Ye[c], Yiping Wei[c], Hua Zhang[a], Konstantin Chingin[d], Vladimir Frankevich[e], Huanwen Chen[b,d,*]

[a] State Key Laboratory of Inorganic Synthesis and Preparative Chemistry, College of Chemistry, Jilin University, Changchun 130012, China
[b] Jiangxi Key Laboratory for Mass Spectrometry and Instrumentation, East China University of Technology, Nanchang 330013, China
[c] The Second Affiliated Hospital of Nanchang University, Nanchang 330006, China
[d] School of Pharmacy, Jiangxi University of Chinese Medicine, Nanchang 330004, China
[e] National Medical Research Center for Obstetrics, Gynecology and Perinatology named after Academician V.I. Kulakov of Ministry of Healthcare of Russian Federation, Moscow 117997, Russian Federation

ARTICLE INFO

Article history:
Received 12 December 2023
Revised 4 May 2024
Accepted 31 May 2024
Available online 2 June 2024

Keywords:
Lung cancer
Tumor margins
Internal extractive electrospray ionization
Mouse models
Postoperative recurrence

ABSTRACT

Accurate determination of lung cancer margins at the molecular level is of great significance to determine the optimal extent of resection during surgical operation and reduce the risk of postoperative recurrence. In this study, internal extractive electrospray ionization mass spectrometry (iEESI-MS) was used to trace potential molecular tumor margins in lung cancer tissue. Molecular differential model for the determination of lung cancer tumor margin was established *via* partial least-squares discriminant analysis (PLS-DA) of iEESI-MS data collected from lung tissue pieces within cancer tumor area and iEESI-MS data collected from lung tissue pieces outside cancer tumor area. Proof-of-concept data demonstrate that the developed molecular differential model yields *ca.* 1–2 mm wider potential molecular tumor margin of a lung cancer compared to the conventional histological analysis, showing promising potential of iEESI-MS to increase the accuracy of tumor margins determination and lower risk of lung cancer postoperative recurrence. Furthermore, our results revealed that creatine and taurine showed positive correlations with lung cancer.

Lung cancer is the leading cause of cancer-related deaths worldwide [1]. It is well accepted that the complete resection of tumor is associated with an improved prognosis for lung cancer [2]. Usually, lung cancer surgical margin is assessed intraoperatively by histological evaluation of multiple frozen sections [3]. Histological evaluation process involves tissue freezing, cryosection, hematoxylin and eosin (H&E) staining, and microscopic examination, this typically takes more than 30 min. Due to the histological examination is a subjective procedure, the results are highly dependent on the skill of technicians and pathologists as well as the quality of frozen sections [3-6]. Fluorescence imaging can be utilized for intraoperative determination of tumor margins with the help of tumor-targeted fluorescence nanoprobes. Nevertheless, conventional fluorescence probes frequently encounter challenges related to poor signal-to-background ratios [7]. Therefore, it is urgent to develop alternative methods for the more accurate, reliable, and real-time intraoperative assessment of tumor margins during lung cancer surgeries. This would be of great benefit in improving surgical outcomes and prognosis, as well as for reducing the risk of postoperative recurrence in lung cancer patients.

In alternative to the standard histopathology methods for the evaluation of tumor margins, molecular analysis driven by mass spectrometry-based techniques has gained increasing attention in tumor margins definition. This is largely because molecular analysis, with high accuracy and sensitivity, provides more information than that may be unavailable in histopathology [8]. The molecular analysis of tumor margins by ambient mass spectrometry (AMS) opens a new perspective to incorporate cancer-specific biomarkers into clinical decision-making for improving the accuracy, specificity and spatial resolution of cancer diagnosis, with the advantages in real-time and direct profiling of molecular information from various biological samples [6,9,10]. For example, desorption electrospray ionization mass spectrometry (DESI-MS) has been employed for the determination of the boundaries between healthy and neoplastic tissues of human brain tumors and glioma based on lipid patterns [11,12]. DESI-MS imaging has been employed for the di-

* Corresponding author.
E-mail address: chw8868@gmail.com (H. Chen).

https://doi.org/10.1016/j.cclet.2024.110077
1001-8417/

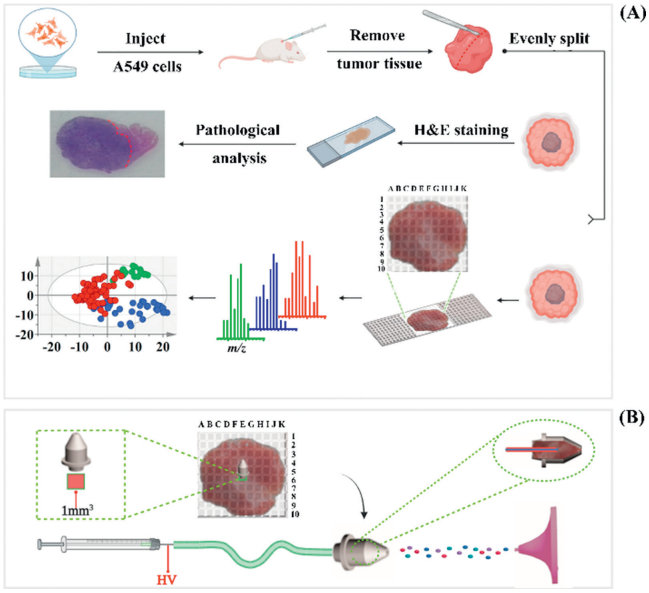

Fig. 1. Experimental workflow for tracing the molecular tumor margin using iEESI-MS. (A) Schematic diagram of operation procedures of cell injection, tissue sample collection, sample grouping, and data processing, (B) disposable iEESI ion source for tissues analysis.

rect molecular assessment of surgical margins of gastric cancer [9] and human medulloblastoma cancers [13]. In addition, the *in vivo* application of rapid evaporative ionization mass spectrometry (REIMS) has been demonstrated in the detection of the tumor margins in brain, liver, lung, breast, or colorectal tumors [14]. More recently system, MasSpec Pen [6] has been demonstrated suitable for tumor margin assessment during pancreatic cancer surgery [15]. These results indicate the huge potential of AMS for the determination of cancer margins. However, DESI-MS mainly obtained surface molecular information, while a large amount of heat is involved in the operation/ionization sampling process of REIMS. Also, the degradation of biological analytes is difficult to avoid, which might cause some information to be lost and eventually introduce uncertainties into the results. MasSpec Pen device must be placed in tight contact with the tissue for analysis. Possible contamination of the device with tissue debris on the analytical results limits its use for cancer research [10,16].

Internal extractive electrospray ionization mass spectrometry (iEESI-MS) [17-20] is an alternative AMS method for the accurate evaluation of lung cancer molecular margin. Like DESI-MS and REIMS, iEESI-MS technology enables direct analysis of tissue samples. Unlike DESI-MS and REIMS, where tissues are typically analyzed online by continually scanning position of the sampling spot, in iEESI-MS every tissue spot is sampled and analyzed separately. Given the necessity for precise control over tissue section thickness in this study, we sliced the tissue sections to a thickness of 1 mm and mounted them onto the slide. Typically, when tissue sample thickness is not a critical factor, sample preparation steps such as fixing and slicing may be unnecessary. The overall workflow of cell injection, tissue sample collecting, sample grouping, and data processing is shown in Fig. 1A. To ensure the reproducibility of our work, we meticulously defined the capacity of the sample chamber, which in turn determined the precise amount of sample loaded into it. As shown in Fig. 1B, the tissue sample was directly loaded into the sampler chamber by applying a single punch with the sampler onto the tissue. Then the sample chamber loaded with the tissue samples were assembled with an iEESI source. The positioning was meticulously controlled, with sampling conducted row by row and column by column. These procedures ensure that each tissue spot undergoes sampling and analysis individually. Such a methodical approach not only maintains uniformity but also enhances the reproducibility of iEESI-MS analysis. The process of iEESI-MS could be briefly described as follows: the extraction solution of CH_3OH/H_2O (v/v, 30/70) charged with +5.0 kV was infused into the tissue samples at 2.0 μL/min through a syringe (250 μL, Hamilton, GR, Switzerland) controlled by a syringe pump (Harvard, MA, USA). This process selectively extracts analytes distributed within the tissue samples, producing gas ions for mass spectrometry profiling. The iEESI-MS approach has been successfully applied for the rapid discrimination of tissue samples from human esophageal squamous cell carcinoma [21], lung cancer [22,23], and liver cancer [24]. While in the earlier works only cancer and normal datasets were used for differentiation analysis. In the present study, we incorporated the data from tissue samples in the tumor margin area (M) to delineate the possible locations of tumor molecular margins. Additionally, we tracked the recurrence of mice following tumor removal based on the conventional pathological method. Our findings revealed that mouse, with *ca.* 1–2 mm wider molecular tumor margins than pathological tumor margins, experienced postoperative recurrence three weeks after tumor removal based on the pathological margins. These results underscore the great potential of iEESI-MS in improving the accuracy of tumor margin determination during lung cancer surgery. Furthermore, our study identified two potential biomarkers, creatine and taurine, which showed positive correlations with lung cancer.

Note that normal tissues used in this study were collected from mice with lung cancers (outside the tumor) rather than from healthy mice without lung cancer. This strategy was employed to delineate the potential molecular margins of lung cancer. The current experiment included a total of 660 tissue samples. The time required for one tissue section is size-dependent. For example, if there are around 50 tissue spots within one tissue section, the whole time is around 30 min. The details of materials and method refer to the Supporting information.

The *m/z* range of 700–900 was used for molecular differentiation as it contains the characteristic band of phospholipids. Phospholipids are integral to a multitude of biological functions including cell signaling, cell-cell recognition, immune response, energy metabolism, and malignant transformation of cells [25,26]. Consequently, investigating phospholipids is of great interest in revealing the essence of life activities. Earlier studies revealed that phospholipids profiles differ between cancerous tissues and normal tissues in lung cancer [22,26] and liver cancer [24]. Fig. S1 (Supporting information) shows the mass spectrum of normal tissues (Fig. S1A) and cancerous tissues (Fig. S1B) of mice obtained on LTQ mass spectrometer. Partial least-squares discriminant analysis (PLS-DA) is chosen over other discriminant analysis methods due to its ability to handle multicollinearity, flexibility, dimensionality-reduction, and its proven success in modeling high-dimensional datasets for disease classification in medical diagnosis [27,28]. As shown in Fig. S2A (Supporting information), normal tissue samples are clearly separated from primary tumor tissue samples. For PLS-DA model, the values of R^2X, R^2Y and Q^2Y were 0.77, 0.68 and 0.64, respectively. Validation with 200 random permutation tests of PLS-DA model generated intercepts $R^2 = 0.19$ and $Q^2 = -0.14$, indicating that the model was not overfitted (Fig. S2B in Supporting information). The iEESI-MS data corresponding to 24 tissue samples in tumor margin area (numbers from 1A to 6D in Fig. S3A in Supporting information) were processed by the PLS-DA differential model (Fig. S2A) to assess lung cancer molecular tumor margin. As shown in Fig. S3B (Supporting information), the PLS-DA plot indicated that 8 tissue samples (Nos. 1A, 2A, 3A, 4A, 5A, 6A, 1B, and 2B) were assigned to normal tissue area, this was consistent with the results of histological analysis. Nevertheless, 3 tissue samples (Nos. 3B, 4B, and 5B) were assigned to cancerous tissue by PLS-

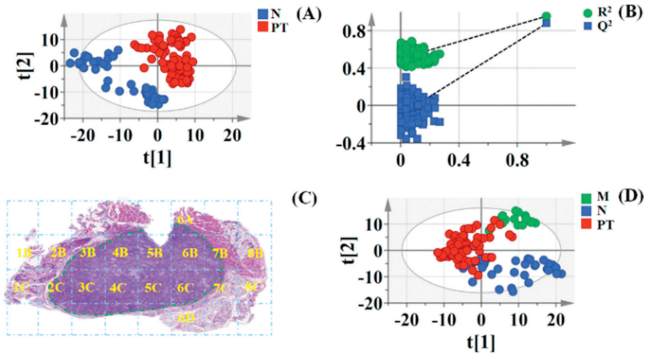

Fig. 2. (A) Score plot of PLS-DA derived from iEESI-MS data of primary tumor (PT, red squares) and normal tissue samples (N, blue squares). (B) Validation of results with 200 permutation tests of PLS-DA model. (C) H&E stains of tissue sections. (Green dotted line indicated pathological tumor margin, and 18 numbers (from 1B to 8C) indicate the sampling location of 18 margin tissue samples). (D) Score plot of PLS-DA derived from iEESI-MS data of primary tumor (PT, red squares), normal (N, blue squares), and margin tissue samples (M, green squares).

DA. The results might suggest *ca.* 1–2 mm larger tumor size compared to the results of histological analysis. Additionally, multi-step screening processes including S-plot, and variable influence on projection (VIP) value revealed that *m/z* 757 $[PC(32:0)+Na]^+$, and *m/z* 783 $[PC(36:4)+H]^+$ have the highest contribution to the molecular differentiation of lung cancer (Fig. S4 in Supporting information).

To increase the reliability of experimental results obtained on LTQ at Nanchang, China, we performed cross-validation experiments on Orbitrap Fusion Tribrid mass spectrometer at Changchun, China. Thirty-seven normal tissue samples and 87 primary tumor tissues samples were used to build the molecular differentiation model using PLS-DA. As shown in Fig. 2A, the primary tumor and normal tissue samples could be completely separated. Validation with 200 random permutation tests of PLS-DA model (Fig. 2B) generated intercepts $R^2 = 0.45$ and $Q^2 = -0.14$, indicating that the model was not overfitted, which could be used for the molecular margin determination. Therefore, the 18 iEESI-MS data points corresponding to 18 tissue points in tumor margin area (numbers from 1B to 8C in Fig. 2C) were then processed by the PLS-DA differential model (Fig. 2A) to trace possible lung cancer molecular margins. It could be observed from Fig. 2D that all data were attributed to the cancer group by PLS-DA model. Interestingly, 5 tissue points, including 1B, 1C, 6D, 8B, and 8C, were diagnosed as normal tissue samples *via* histological analysis. This molecular analysis result suggests *ca.* 1–2 mm larger tumor size compared to the results of histological analysis. It is worth to be mentioned that mouse, with *ca.* 1–2 mm wider molecular tumor margins than pathological tumor margins, experienced postoperative recurrence three weeks after tumor removal according to the pathological margin, this further indicated that tumor removal based on molecular tumor margins might be helpful for the lower risk of tumor recurrence. Note that some single 1 mm square tissue points used for iEESI-MS might cross the boundary of a cancer tissue. In other words, both normal and caner tissues could exist in some tissue points. Thus, final analysis results may be biased if only depending on the percentage of cancer tissue over normal tissues.

Herein we also compared the molecular difference among normal, primary tumor, and recurrent tumor tissue samples. As shown in Fig. S5 (Supporting information), a variety of ions were detected from normal (Fig. S5A), primary tumor (Fig. S5B) and recurrent tumor tissues (Fig. S5C). The predominant peaks at mass range of *m/z* 100–1000 were identified as *m/z* 148.0040 $[Taurine+H]^+$, *m/z* 162.1128 $[L\text{-}Carnitine+H]^+$, *m/z* 741.5335 $[SM(34:1)+K]^+$, *m/z* 756.5530 $[PC(34:3)+H]^+$, *m/z* 772.5280 $[PC(32:0)+H]^+$, *m/z* 782.5690 $[PC(36:4)+H]^+$. Chemical assignment for the 22 confidently identified species from the tissue sample using iEESI-MS/MS is shown in Table S1 (Supporting information). Here, the inconsistency in positive and negative deviations of the results in Table S1 can be attributed to different mass spectrometry measurements. The predominant compound assignments were based on high-resolution MS data, collision-induced dissociation (CID) experiments, as well as human metabolome database. Note that the MS profiles recorded from the normal tissues (Fig. S5A) were significantly different from those recorded using the primary tumor (Fig. S5B) and recurrent tumor tissues (Fig. S5C). For example, many peaks with −44 Da mass difference were detected at mass range of *m/z* 500–1000 in the mass spectra of normal tissues, while peaks with −44 Da mass difference were detected at mass range of *m/z* 400–600 in the mass spectra of recurrent tumor tissues. For primary tumor tissues, it mainly detected lipids species at mass range of *m/z* 700–900, including *m/z* 741.5335 $[SM(34:1)+K]^+$, *m/z* 756.5530 $[PC(34:3)+H]^+$, *m/z* 772.5280 $[PC(32:0)+H]^+$, and *m/z* 782.5690 $[PC(36:4)+H]^+$. Although both primary tumor and recurrent tumor tissues detected many lipids species at the mass range of *m/z* 700–900, subtle differences exist in the relative abundance.

Previous studies confirmed that the molecular information obtained by iEESI-MS is diagnostic and predictive of disease state [22,24], hence the iEESI-MS data obtained from 174 tissue samples (including 37 normal tissue samples, 87 primary tissue samples, and 50 recurrent tumor tissue samples) were subjected to PLS-DA for differentiation of molecular differences among different types of samples. As shown in Fig. 3, the score plots of PLS-DA among recurrent tumor and primary tumor tissues (Fig. 3A), as well as recurrent tumor and normal tissues (Fig. 3B) exhibited a clear separation. In addition, leave one out cross-validation (LOOCV) revealed that the PLS-DA models among recurrent tumor and primary tumor tissues (Fig. 3C), as well as recurrent tumor and normal tissues (Fig. 3D) had robust cross validation scores (R^2 value = 0.98, Q^2 value > 0.93, accuracy > 0.98), suggesting that the established PLS-DA models had a good explanatory ability and prediction ability. Due to the potential biomarkers contributed to the recurrence of lung cancer are very helpful for offering new therapeutic approaches for limiting tumor recurrence. Through the *t*-test, 1180 and 1126 features, with $P < 0.05$ and a false discovery rate (FDR) <0.05, were identified between recurrent tumor and normal tissues (RT + N), as well as between recurrent tumor and primary tumor tissues (RT + PT), respectively. Venn diagram (Fig. S6 in Supporting information) showed that 558 identified features were shared between RT + N group and RT + PT group. Twenty-one out of 558 confidently identified metabolites (Table S1) were performed enrichment analysis (Fig. 3E), results indicated that these metabolites mainly involved in 13 metabolic pathways, such as spermidine and spermine biosynthesis, arginine and proline metabolism, biotin metabolism, glycine and serine metabolism, and taurine and hypotaurine metabolism. Two altered metabolic pathways, specifically arginine and proline metabolism, as well as taurine and hypotaurine metabolism, were revealed in pathway analysis of data derived from mouse inoculated subcutaneously with A549 lung cancer cells using air-flow assisted desorption electrospray ionization mass spectrometry imaging (AFA-DESI-MSI) [29]. This underscores the potential of iEESI-MS technology in molecular diagnosis of lung cancer. Note that since L-carnitine in Table S1 showed no significant difference between RT + N group and RT + PT group, it is excluded when performing enrichment analysis.

Furthermore, using the Network Explorer module from MetaboAnalyst 5.0, we created metabolite-disease interaction networks to identify connections that cross pathway boundaries among 21 significantly changed metabolites. As shown in Fig. 4A, creatine and taurine showed positive correlations with lung cancer. Boxplots of creatine (Fig. 4B) and taurine (Fig. 4C) showed upregulated levels

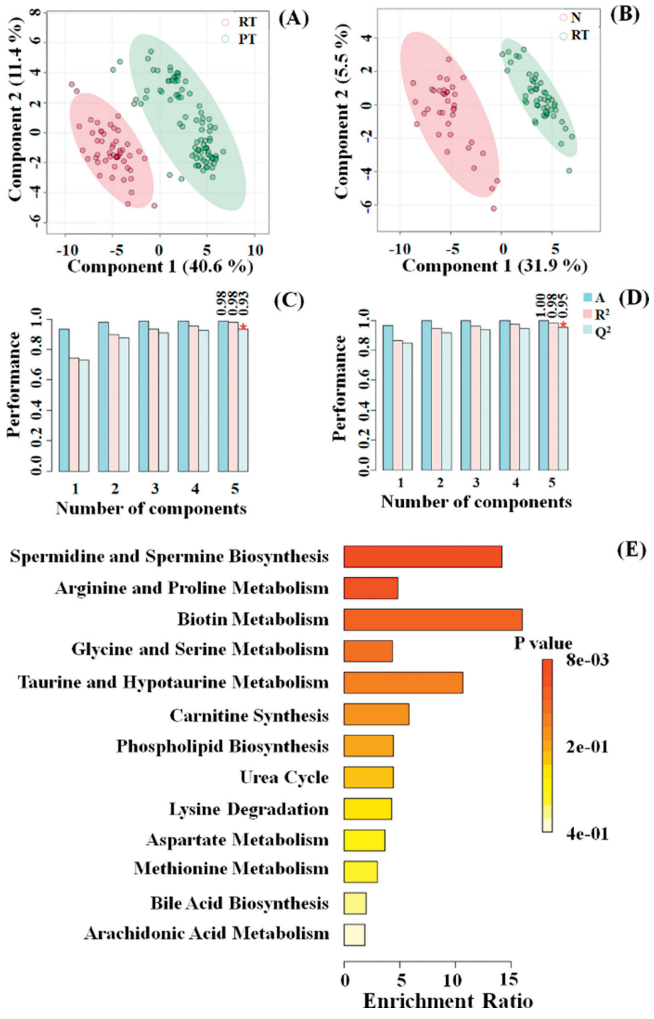

Fig. 3. Score plot of PLS-DA of (A) recurrent tumor and primary tumor tissues, (B) recurrent tumor and normal tissues. LOOCV of PLS-DA model of (C) recurrent tumor and primary tumor tissues, and (D) recurrent tumor and normal tissues (A, R^2, and Q^2 indicated accuracy, the explained variance, and the predictive capability of the model, respectively). (E) Metabolites enrichment analysis of 21 confidently identified metabolites between recurrent tumor and primary tumor tissues as well as recurrent tumor and normal tissues. Note: RT, PT and N indicated recurrent tumor, primary tumor, and normal tissues, respectively.

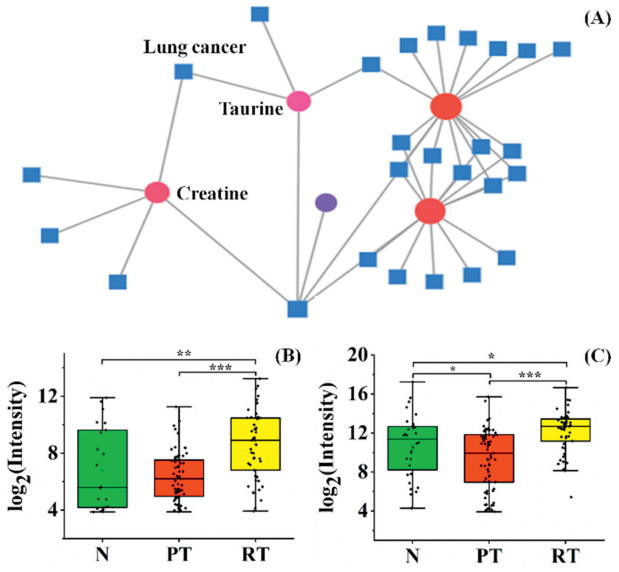

Fig. 4. (A) Metabolite-disease interaction network analysis of shared 21 confidently identified metabolites within recurrent tumor and normal tissue group, as well as recurrent tumor and primary tumor tissue group) (Enriched terms are represented as nodes, and the node size represents the significance for each term. Circles represent one metabolite and squares an associated disease). Boxplot of creatine (B) and taurine (C) among normal (N), primary tumor (PT) and recurrent tumor (RT) tissue samples. Box plots demarcate the median line, the 25th and 75th percentile (box), and 1.5 times the interquartile range (whiskers). Significant difference was determined by a two-tailed *t*-test ($^{*}P < 0.05$, $^{**}P < 0.01$, and $^{***}P < 0.001$).

in the recurrent tumor tissues compared to that in the normal and primary tumor tissues.

Tumor surgery implies the removal of an apparently non-tumorous tissue around the tumor to reduce recurrence chances [30]. From this regard, accurate identification of resection margins plays a critical role in lowering cancer recurrence risk. Our results indicated that iEESI-MS combined with PLS-DA molecular differentiation model revealed that there was a potential molecular tumor margin *ca.* 1–2 mm wider than histological tumor margin. This suggests that iEESI-MS analysis may be more sensitive to the occurrence of cancer in margin areas. Especially, consistent results between LTQ mass spectrometers at Nanchang, China and Orbitrap Fusion Tribrid mass spectrometer at Changchun, China further provided solid support that molecular tumor margins were wider *ca.* 1–2 mm compared to the conventional histological tumor margins. Taken together, our results further highlighted that the development of novel molecular diagnosis methods plays a critical role in lowering the risk recurrence of lung cancer.

Moreover, metabolite-disease interaction networks analysis highlighted that creatine and taurine showed positive correlations with lung cancer. Aberrant levels of metabolites are associated with cancer progression, which could potentially be used for diagnosis or indicators for therapeutic evaluation [31]. Boxplot in Fig. 4 showed that creatine and taurine were upregulated in the recurrent tumor tissues compared to that in the normal and primary tumor tissues. Creatine is a nitrogen-containing organic acid and can be converted into phosphocreatine to provide energy for muscle and nerve tissues [31]. Compared the expression levels of creatine among normal, primary tumor, and recurrent tumor tissues, creatine showed an up-regulated level both in primary tumor and recurrent tumor tissues, this is consistent with previous report that the mean concentration of creatine significantly increased in lung cancer patients compared with non-diseased controls in urine and serum samples [32]. Taurine is a non-protein amino acid, and influences various cellular functions, such as osmoregulation, antioxidation, and ion movement [33]. Previous study found that lung cancer patients with high serum taurine levels generally responded to PD-1 blockade antibody therapy, suggesting that taurine could serve as a potential therapeutic agent for lung cancer patients [34]. Taken together, these findings in respect to aberrant levels of creatine and taurine will aid in the elucidation of the mechanisms of lung cancer pathogenesis. Furthermore, we are continuing to explore these differential features revealed by PLS-DA, with the aim of discovering more potential biomarkers and performing further validation of their specific role in lung cancer pathology. Based on the previous successful application of iEESI-MS in quantitative determination of bulk molecular concentrations of β-agonists in pork tissue samples [20] and amino acids in tissues for the assessment of lung cancer [23], we are going to utilize this method to quantitatively and specifically identify biomarkers associated with lung cancer to enhance its accuracy and specificity in molecular diagnosis of lung cancer margins.

In conclusion, the proof-of-concept data demonstrate that the iEESI-MS technology coupled with PLS-DA could be used to determine molecular tumor margins *via* mice with lung cancer through

metabolites profiling with *ca.* 1 mm spatial resolution. The result indicate that potential molecular tumor margins are *ca.* 1–2 mm wider than histological tumor margins, highlighting the great potential of iEESI-MS approach for the objective determination of lung cancer margin with higher accuracy and sensitivity compared to the conventional histological analysis. However, major efforts should be focused on spatial resolution and potential misalignment of the histological image and annotation with the iEESI pixels in the following work, with aim at increasing the accuracy of tumor margins determination during lung cancer surgery and lowering the cancer recurrence risk. Further validation studies (such as comparison analysis between frozen sections and iEESI-MS) are required to determine the accuracy of iEESI-MS for intraoperative oncological margin assessment in the future work.

Ethical statement

All animal treatment and experiments were conducted according to the ethical guidelines for laboratory animal use and approved by the Medical Research Ethics Committee of the Second Affiliated Hospital of Nanchang University.

Declaration of competing interest

The authors declare that they have no known competing financial interests or personal relationships that could have appeared to influence the work reported in this paper.

CRediT authorship contribution statement

Haiyan Lu: Data curation, Writing – original draft. **Jiayue Ye:** Data curation, Formal analysis, Methodology, Writing – original draft. **Yiping Wei:** Formal analysis, Methodology, Writing – review & editing. **Hua Zhang:** Data curation, Methodology. **Konstantin Chingin:** Investigation, Methodology, Writing – review & editing. **Vladimir Frankevich:** Methodology, Writing – review & editing. **Huanwen Chen:** Conceptualization, Funding acquisition, Project administration, Supervision, Writing – review & editing.

Acknowledgments

This work was supported by Jiangxi Provincial International Science and Technology Cooperation Project (Nos. 20203BDH80W010 and 20232BBH80012), the National Natural Science Foundation of China (Nos. 82160410 and 81860379), Foundation of Jiangxi Provincial Department of Science and Technology (No. 20212ACB206018), and Key Research and Development Program of Jiangxi Province (No. 20223BBG71009).

Supplementary materials

Supplementary material associated with this article can be found, in the online version, at doi:10.1016/j.cclet.2024.110077.

References

[1] H. Sung, J. Ferlay, R.L. Siegel, et al., CA Cancer J. Clin. 71 (2021) 209–249.
[2] P. Goldstraw, K. Chansky, J. Crowley, et al., J. Thorac. Oncol. 11 (2016) 39–51.
[3] J.D. Predina, J. Keating, N. Patel, et al., J. Surg. Oncol. 113 (2016) 264–269.
[4] V. Pirro, R.S. Llor, A.K. Jarmusch, et al., Analyst 142 (2017) 4058–4066.
[5] K. Ashizawa, K. Yoshimura, H. Johno, et al., Oral Oncol. 75 (2017) 111–119.
[6] J.L. Zhang, J. Rector, J.Q. Lin, et al., Sci. Transl. Med. 9 (2017) eaan3968.
[7] J. Xin, S. Han, M. Zheng, et al., Chin. Chem. Lett. 35 (2024) 109165.
[8] H.M. Brown, V. Pirro, R.G. Cooks, Clin. Chem. 64 (2018) 628–630.
[9] L.S. Eberlin, R.J. Tibshirani, J. Zhang, et al., Proc. Natl. Acad. Sci. U.S.A. 111 (2014) 2436–2441.
[10] H. Lu, H. Zhang, Y. Wei, et al., Analyst 145 (2020) 313–320.
[11] L.S. Eberlin, I. Norton, D. Orringer, et al., Proc. Natl. Acad. Sci. U.S.A. 110 (2013) 1611–1616.
[12] V. Pirro, C.M. Alfaro, A.K. Jarmusch, et al., Proc. Natl. Acad. Sci. U.S.A. 114 (2017) 6700–6705.
[13] L. Katz, M. Woolman, F. Talbot, et al., Anal. Chem. 92 (2020) 6349–6357.
[14] J. Balog, L. Sasi-Szabo, J. Kinross, et al., Sci. Transl. Med. 5 (2013) 194ra93.
[15] M.E. King, J. Zhang, J.Q. Lin, et al., Proc. Natl. Acad. Sci. U.S.A. 118 (2021) e2104411118.
[16] P. Saudemont, J. Quanico, Y.M. Robin, et al., Cancer Cell 34 (2018) 840–851.
[17] H. Zhang, K. Chingin, L. Zhu, et al., Anal. Chem. 87 (2015) 2878–2883.
[18] H. Zhang, L. Zhu, L. Luo, et al., J. Agric. Food Chem. 61 (2013) 10691–10698.
[19] H. Zhang, H. Gu, F. Yan, et al., Sci. Rep. 3 (2013) 2495.
[20] J. Xu, S. Xu, Y. Xiao, et al., Anal. Chem. 89 (2017) 11252–11258.
[21] J. Zhang, J. Xu, Y. Ouyang, et al., Sci. Rep. 7 (2017) 3738.
[22] H. Lu, H. Zhang, K. Chingin, et al., Anal. Chem. 91 (2019) 10532–10540.
[23] H. Lu, Y. Li, H. Zhang, et al., Talanta 233 (2021) 122544.
[24] H. Lu, H. Zhang, Y. Xiao, et al., Analyst 145 (2020) 6470–6477.
[25] H. Zhang, K. Chingin, J. Li, et al., Anal. Chem. 90 (2018) 12101–12107.
[26] H.-Y. Lu, J.-Y. Zhang, W. Zhou, et al., Chin. J. Anal. Chem. 44 (2016) 329–334.
[27] L.C. Lee, C.Y. Liong, A.A. Jemain, Analyst 143 (2018) 3526–3539.
[28] D. Ruiz-Perez, H. Guan, P. Madhivanan, et al., BMC Bioinf. 21 (2020) 2.
[29] J. Huang, S. Gao, K. Wang, et al., Chin. Chem. Lett. 34 (2023) 107865.
[30] F.G. Almeida, P.F. de Aquino, S.R. Chalub, et al., J. Proteomics 154 (2017) 59–68.
[31] L. Zhang, P. Bu, Trends Cell Biol. 32 (2022) 380–390.
[32] D.P. Patel, G.T. Pauly, T. Tada, et al., J. Pharm. Biomed. Anal. 191 (2020) 113596.
[33] T. Qaradakhi, L.K. Gadanec, K.R. McSweeney, et al., Nutrients 12 (2020) 2847.
[34] Y. Ping, J. Shan, Y. Liu, et al., Cancer Immunol. Immunother. 75 (2022) 1015–1027.